

## Enhanced $\gamma$ vibration and a Long-lived $K$ isomer in axially symmetric $^{172}\text{Dy}$

---

**Hiroshi Watanabe\***

*IRCNPC, School of Physics, Beihang University*

*E-mail: hiroshi@ribf.riken.jp*

*The 26th International Nuclear Physics Conference  
11-16 September, 2016  
Adelaide, Australia*

---

\*Speaker.

## 1. Introduction

The  $\gamma$  vibration is one type of quadrupole shape oscillation in well-deformed nuclei, which causes an instantaneous breaking of axial symmetry. Experimentally, the existence of low-lying  $\gamma$ -vibrational band built on the  $K^\pi = 2^+$  band head ( $K$  denotes the angular-momentum projection on the symmetry axis) can serve as a signature of enhanced non-axial quadrupole collectivity. In this contribution, we will focus on the first spectroscopic results of the ground-state (g.s.) and  $\gamma$ -vibrational bands in  $^{172}\text{Dy}$ , the most neutron-rich Dy isotope studied to date [1]. Its excited states have been populated through the decay from a long-lived isomer, which has the same configuration as the  $K^\pi = 8^-$  isomers that had been identified in the  $N = 106$  isotones from  $Z = 68$  to 82 [2]. It is notable that high- $K$  isomers can serve as a useful probe for the underlying nuclear structure since their nature is sensitive to intrinsic orbits near the Fermi surface, pairing and other residual interactions, and the degree of axial symmetry [3].

## 2. Experimental procedures

Neutron-rich nuclei around  $A = 170$  were produced by in-flight fission of a  $^{238}\text{U}^{86+}$  beam at 345 MeV/u with an average intensity of 12 pnA. The nuclei of interest were separated and identified through the BigRIPS separator [4]. For purification of the secondary beams, wedge-shaped aluminium degraders with thicknesses of 4.5 and 1.0 mm were installed at the first (F1) and second (F5) dispersive focal planes, respectively. Identification of particles with the atomic number ( $Z$ ) and the mass-to-charge ratio ( $A/q$ ) was achieved on the basis of the  $\Delta E$ -TOF- $B\rho$  method, in which the energy loss ( $\Delta E$ ), time of flight (TOF), and magnetic rigidity ( $B\rho$ ) were measured using the focal-plane detectors on the beam line. The secondary beams were transported with two different settings of the slits on the beam line; one is optimized for  $^{170}\text{Dy}^{66+}$ , and the other for  $^{172}\text{Dy}^{66+}$ . The resolution of the mass-to-charge ratio ( $\lesssim 0.05\%$ ) was sufficient to separate nearby hydrogen-like ions. The identified particles were implanted into WAS3ABi [5], which consisted of two layers of double-sided silicon-strip detectors (DSSSD) stacked compactly. Each DSSSD had a thickness of 1 mm with an active area segmented into sixty and forty strips (1-mm pitch) on each side in the horizontal and vertical dimensions, respectively. The DSSSDs also served as detectors for electrons following  $\beta$ -decay and internal conversion (IC) processes. Gamma rays were detected by the EURICA spectrometer [5]. The  $\gamma$ -ray measurements were carried out within a time range up to 100  $\mu\text{s}$  relative to the trigger signal generated either from a plastic scintillation counter placed at the end of the beam line or from WAS3ABi. About  $7.1 \times 10^3$   $^{172}\text{Dy}$  ions were implanted into WAS3ABi during the experiment.

The beam, electron, and  $\gamma$ -ray events were time-stamped and recorded by independent data-acquisition systems. For the analysis of beam- $\gamma$  delayed coincidence, the  $\gamma$ -ray data sets were combined with those of the beam particles on an event-by-event basis using information on the time stamp. Isomeric states with (sub)microsecond lifetimes were identified with appropriate time gates. Meanwhile, all data sets containing beam, electron, and  $\gamma$ -ray events were used for  $\beta$ - $\gamma$  and IC- $\gamma$  coincidence analyses, in which the implantation of an identified particle was associated with the subsequent electron events that were detected in a given correlation area in the DSSSDs where

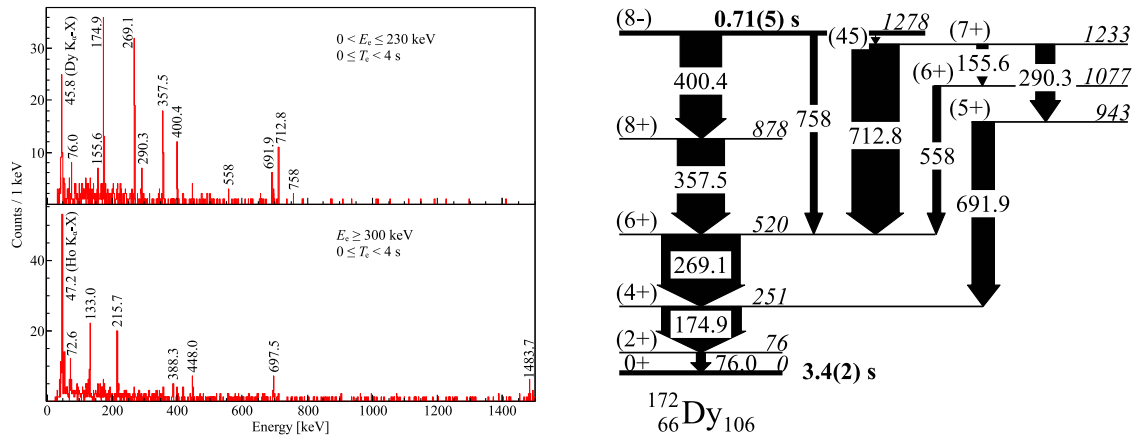


**Figure 1:** Left:  $\gamma$ -ray energy spectra measured with gates on electron energy ( $E_e$ ) and time ( $T_e$ ) as indicated after implantation of  $^{172}\text{Dy}$  ions. Right: partial level scheme of  $^{172}\text{Dy}$  constructed in the present work.

the beam particle was implanted. Decay half-lives ( $T_{1/2}$ ) in the millisecond range were extracted from the time distributions of  $\gamma$ -ray gated electron events with respect to the fragment implantation.

### 3. Results

There was no spectroscopic information on the excited states of  $^{172}\text{Dy}$  before the present work. The  $\gamma$ -ray energy spectrum shown in the upper left of Fig. 1 was measured within 4 s after the implantation of  $^{172}\text{Dy}$  with a gate on an electron energy ranging from 0 to 230 keV. Since such low-energy signals arise predominantly from IC electrons rather than from  $\beta$  particles, the  $\gamma$  transitions observed under this gate condition can be associated with the decay from a long-lived isomer in the implanted nucleus. The measured X-ray energy at 45.8 keV is in good agreement with the  $K_\alpha$  lines for Dy atoms.

The level scheme of  $^{172}\text{Dy}$  established in the present work is displayed in the right panel of Fig. 1. In the  $A \sim 170$  region of interest, the level sequence of the g.s. rotational band in even-even nuclei is similar to that of the neighboring isotopes and unlikely to change drastically with the proton or neutron number. Therefore, based on the systematics for lighter Dy isotopes and heavier  $N = 106$  isotones, the transitions of 76, 175, 269, and 358 keV are assigned as  $2_1^+ \rightarrow 0_1^+$ ,  $4_1^+ \rightarrow 2_1^+$ ,  $6_1^+ \rightarrow 4_1^+$ , and  $8_1^+ \rightarrow 6_1^+$ , respectively. The latter three transitions are found to be in mutual coincidence. Based on this, we propose a state at 1278 keV as a  $K^\pi = 8^-$  isomer, which feeds the  $8_1^+$  level via a hindered  $E1$  transition, consistent with what was observed for the heavier  $N = 106$  isotones [2].

In addition to the 400-358-269-175-76-keV cascade, several other  $\gamma$  rays are visible in Fig. 1. A weak  $\gamma$  ray at 758 keV is assigned as a  $M2$  branch from the  $8^-$  isomer to the  $6_1^+$  state on account of the consistency in energy with the sum of 400 and 358 keV. Gamma-gamma coincidence analyses reveal that the  $\gamma$  ray at 713 keV is in coincidence with the 175- and 269-keV transitions, but neither with the 358- nor 400-keV transitions, while the 290- and 692-keV  $\gamma$  rays are in mutual coincidence and with the 175-keV line. The energy matching for these cascades suggests the presence of a 45-keV transition from the 1278-keV isomer to an intermediate state at 1233 keV, though the

corresponding  $\gamma$  line could not be separated from the intense Dy  $K_\alpha$  -X ray. The placement of the 1233-keV state below the  $8^-$  isomer is additionally supported by the observation of  $\gamma$  rays at 156 and 558 keV, the sum of their energies in agreement with 713 keV within errors. The orders of the 290-692- and 156-558-keV transitions could not be determined from the present analysis of  $\gamma$ - $\gamma$  coincidence and  $\gamma$ -ray intensity. However, the proposed sequence of the non-yrast levels in Fig. 1 are justified based on the arguments of the moment of inertia and the decay pattern towards the g.s. rotational band. A half-life of 0.71(5) s has been derived from a least-squares fit of the summed  $\gamma$ -ray gated time spectra for the isomeric-decay transitions. More details on the data analysis are described in Ref. [1].

Spins of 5, 6, and 7 are tentatively assigned for the states at 943, 1077, and 1233 keV, respectively, based on the observed feeding patterns towards the members of the g.s. rotational band. Concerning the parity of these levels, if they had negative parity, the  $K^\pi = 8^-$  isomer would preferentially decay towards the 1077-keV state via an  $E2$  transition. Because such a  $\gamma$  ray has not been observed in this experiment, we propose positive parity to these levels. Essentially, in all deformed even-even nuclei, the non-yrast level sequence with positive parity, including odd-spin states, below the pairing-gap energy,  $2\Delta \sim 1.5$  MeV, is the best candidate for a  $K^\pi = 2^+$   $\gamma$ -vibrational band. With this as an assumption, the moment of inertia for the 290-keV,  $(7_1^+) \rightarrow (5_1^+)$  transition is estimated to be  $44.8 \hbar^2 \text{MeV}^{-1}$ . This is somewhat larger than that of the g.s. band at low rotational frequencies, 39.5 ( $2_1^+ \rightarrow 0_1^+$ ), 40.0 ( $4_1^+ \rightarrow 2_1^+$ ), 40.9 ( $6_1^+ \rightarrow 4_1^+$ ),  $42.0 \hbar^2 \text{MeV}^{-1}$  ( $8_1^+ \rightarrow 6_1^+$ ), as is also found for the neighboring even-even nuclei, supporting the assignment of the  $\gamma$ -band levels. The energies of unpopulated lower-spin members are estimated to be 671 ( $2_\gamma^+$ ), 739 ( $3_\gamma^+$ ), and 830 keV ( $4_\gamma^+$ ) from an extrapolation of the  $\gamma$ -band levels based on the standard rotational-energy equation,  $E(J) = E_0 + A[J(J+1) - K^2] + B[J(J+1) - K^2]^2$ , where A and B represents the rotational-band parameters.

The proposed  $\gamma$ -band levels are found to preferentially decay towards the g.s. rotational band rather than its lower-spin members. According to the concept of  $\Delta K = 2$  mixing between the g.s. and  $\gamma$ -vibrational bands, in the present case, a competing in-band  $E2$  transition to the possible  $3_\gamma^+$  state is expected to have a  $\gamma$ -ray intensity of 4.3 % relative to the  $5_\gamma^+ \rightarrow 4_g^+$  inter-band transition [1]. This fraction would be hard to be observed with the present statistics.

Besides the internal decay branches, the  $T_{1/2} = 0.71$  s isomer decays externally towards the daughter nucleus  $^{172}_{67}\text{Ho}_{105}$ . The lower left panel in Fig. 1 shows a  $\gamma$ -ray energy spectrum measured by gating on an electron energy of 300 keV and higher, where  $\beta$  rays are predominant over IC electrons, as is evident from the observation of the Ho  $K_\alpha$ -X ray at 47.2 keV. It turns out that the 216-keV  $\gamma$  ray disappears for the longer time range (see Fig. 1(j) in Ref. [1]). The other  $\gamma$  rays at 73, 133, 388, 448, 698, and 1484 keV are believed to arise from the  $\beta$  decay of the  $^{172}\text{Dy}$  ground state, which has a longer half-life ( $T_{1/2} = 3.4(2)$  s) than the isomer. Meanwhile, the 216-keV transition, which exhibits a similar time behavior to the internal decay branches, is expected to follow the  $\beta$  decay from the  $K^\pi = 8^-$  isomer. The  $\beta$ -decay branching ratio from the  $^{172}\text{Dy}$  isomer is estimated to be 19(3) % with the assumption that all the  $\beta$ -decay intensity flows into the 216-keV transition. The measured  $\beta$ -branching ratio yields  $\log ft = 5.0(2)$  using  $T_{1/2} = 0.71(5)$  s and  $Q_\beta = 3470(360)$  keV. Note that this  $\log ft$  value is obtained for a possible  $\beta$  feeding directly towards an excited state at 216 keV in  $^{172}\text{Ho}$ ; in case the state to which the 216-keV transition decays is *not* the ground state, the  $\log ft$  value becomes smaller as its excitation energy increases.

The observation of the small  $\log ft$  value indicates the occurrence of an allowed  $\beta$  transition from the  $K^\pi = 8^-$  isomer, which arises from the neutron 2 quasiparticle (qp) configuration,  $\nu 7/2^- [514] \otimes \nu 9/2^+ [624]$  [2]. It is expected that Gamow-Teller (GT) type  $\beta^-$  decay from this configuration involves the transformation of the  $\nu 7/2^- [514]$  neutron to a proton in the  $\pi 9/2^- [514]$  or  $\pi 7/2^- [523]$  orbital. The former combination of proton and neutron, which satisfies the selection rule of the asymptotic quantum number,  $\Delta N = \Delta n_z = \Delta \Lambda = 0$  and  $\Delta K = 1$ , is known as an allowed-unhindered (au) transition, while the latter is categorized into allowed-hindered (ah)  $\beta$  decay [6, 7]. In the present case of the daughter nucleus  $^{172}\text{Ho}$ , the au state with the  $K^\pi = 9^-$ ,  $\pi 9/2^- [514] \otimes \nu 9/2^+ [624]$  configuration is speculated to be at least 1 MeV higher than the  $K^\pi = 8^-$ ,  $\pi 7/2^- [523] \otimes \nu 9/2^+ [624]$ , ah level, based on the energy difference between the  $K^\pi = 7/2^-$  ground state and the  $K^\pi = 9/2^-$  band head in the well-deformed odd- $A$  Ho isotopes. Here, the ground state of  $^{172}\text{Ho}$  most likely arises from the  $\pi 7/2^- [523] \otimes \nu 7/2^- [514]$  configuration, since these proton and neutron orbitals are assigned as the ground states of the nearby odd- $A$  Ho and  $N = 105$  nuclei, respectively. According to the Gallagher-Moszkowski rule [8], the  $K^\pi = 0^+$  coupling is favored for the ground state of  $^{172}\text{Ho}$ , while the  $K^\pi = 7^+$  partner is likely to be an isomeric state at low excitation energy that undergoes the  $\beta$  decay towards the granddaughter nucleus  $^{172}\text{Er}$ . The presence of a high-spin,  $\beta$ -decaying isomer in  $^{172}\text{Ho}$  is supported by the previous observation of  $\beta$ -delayed  $\gamma$  rays of 138 and 219 keV [9], which were recently assigned as the transitions de-exciting a  $K^\pi = (7^-)$  state in  $^{172}\text{Er}$  [10]. Based on these arguments, it is reasonable to consider that the 216-keV  $\gamma$  ray observed following the  $\beta$  decay of the  $K^\pi = 8^-$  isomer of  $^{172}\text{Dy}$  corresponds to the transition from the  $K^\pi = 8^-$  ah state to the possible  $K^\pi = 7^+$   $\beta$ -decaying isomer in  $^{172}\text{Ho}$ . The energy of the corresponding  $E1$  transition is inferred to be within the range of 100–400 keV from the energy difference between the  $K^\pi = 7/2^- [514]$  and  $9/2^+ [624]$  states in the  $N = 105, 107$  isotones, being comparable to the 216-keV transition. As for the strength of the proposed GT resonances in the proximity of  $^{172}\text{Dy}$ , the au decay has been observed for the  $7/2^- \rightarrow 9/2^-$  transitions in  $^{175}\text{Yb}_{105} \rightarrow ^{175}\text{Lu}_{104}$  and  $^{173}\text{Er}_{105} \rightarrow ^{173}\text{Tm}_{104}$  with  $\log ft = 4.44$  and 4.5, respectively, while the  $7/2^- \rightarrow 7/2^-$  transition with  $\log ft = 5.7$  in  $^{173}\text{Er} \rightarrow ^{173}\text{Tm}$  is ascribed to the ah  $\beta$  decay. The present value of  $\log ft = 5.0(2)$  for the  $^{172m}\text{Dy} \rightarrow ^{172}\text{Ho}$  decay is somewhat smaller than the ah case, due presumably to less occupancy of the  $\pi 9/2^- [514]$  orbital in the Ho isotopes than in Tm. However, further spectroscopic studies will be necessary to conclude this decay channel.

#### 4. Discussion

In the  $N = 106$  isotones, the energies of the  $K^\pi = 8^-$  isomers, which are interpreted as arising from the same neutron 2qp configuration,  $\nu 7/2^- [514] \otimes \nu 9/2^+ [624]$  [11], decrease when the proton number decreases to  $Z = 70$  (Yb) and subsequently rise towards  $^{172}\text{Dy}$ , as shown in Fig. 2(a). The energy systematics from  $^{184}\text{Pt}$  to  $^{174}\text{Er}$  can be understood in terms of the variation of the neutron pairing strength [2]. The isomerism is essentially ascribed to the large difference in the  $K$  quantum number between the isomer and the states to which the isomer decays. For the  $E1$  transition from the  $K^\pi = 8^-$  isomer to the  $8_1^+$  state in the  $K^\pi = 0^+$  g.s. band, which has forbiddenness  $\nu = \Delta K - \lambda = 7$  ( $\lambda$  is the multipolarity), the so-called reduced hindrances,  $f_\nu = (T_{1/2}^\gamma/T_{1/2}^W)^{1/\nu}$ , where  $T_{1/2}^\gamma$  and  $T_{1/2}^W$  represent the partial half-life and the Weisskopf estimate, respectively, increase from 28 in  $^{188}\text{Pb}$  to 98 in  $^{174}\text{Er}$  [see Fig. 2(b)]. The present result of  $^{172}\text{Dy}$ ,  $f_\nu = 133(8)$ , follows

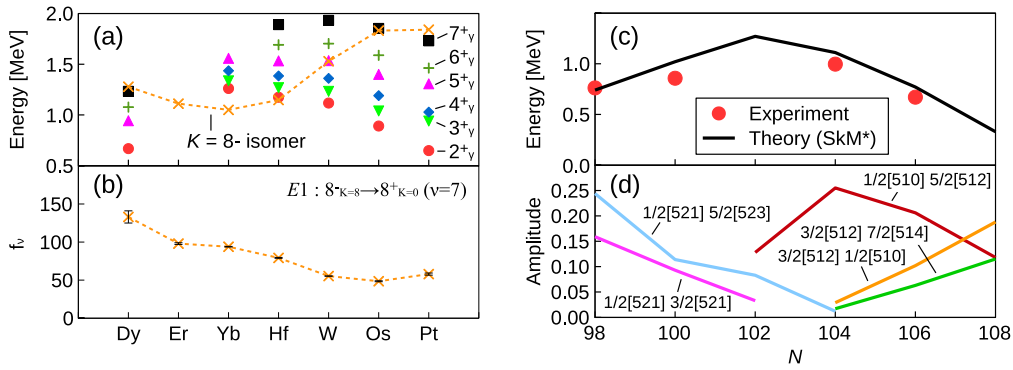


**Figure 2:** (a): Energy systematics of the  $\gamma$ -vibrational bands and  $K^\pi = 8^-$  isomers, and (b): reduced hindrances for the  $E1$  transition from the  $K^\pi = 8^-$  isomer to the  $8_1^+$  state in  $N = 106$  isotones. Dashed lines connecting the data points are a guide to the eye. (c): Energies of the  $K^\pi = 2^+$   $\gamma$ -vibrational band heads. The results of QRPA calculations using the SkM\* functional are also depicted. (d): Amplitudes squared of the neutron 2qp components in the QRPA wave functions for the  $\gamma$ -vibrational mode. The  $2_\gamma^+$  energy of  $^{172}\text{Dy}$  is extrapolated from the observed  $\gamma$ -vibrational levels.

the upward trend in the  $N = 106$  isotones, implying that the  $K$  quantum number is rather robust, as expected for well-deformed axially symmetric nuclei.

It is noteworthy that in the  $N = 106$  isotonic chain the  $\gamma$ -vibrational states abruptly fall in energy in  $^{172}\text{Dy}$ , compared to the corresponding levels in  $^{176}\text{Yb}$  and  $^{178}\text{Hf}$ , as seen in Fig. 2(a). (The  $\gamma$  band has not been identified in the intervening isotope  $^{174}\text{Er}$  to date.) Indeed, the extrapolated energy of the  $2_\gamma^+$  state in  $^{172}\text{Dy}$  is as low as that in the transitional nucleus  $^{184}\text{Pt}$ , which reveals the energy staggering in the low-spin  $\gamma$ -band levels that is characteristic of a  $\gamma$ -unstable nucleus. In general, the lowering of the  $K^\pi = 2^+$   $\gamma$  band would invoke an enhancement of axial asymmetry, which most likely causes  $K$ -mixing in the final states, and therefore, results in a significant reduction of  $f_v$ . For example, anomalously low  $f_v$  values ( $\lesssim 10$ ) have been reported for typical  $\gamma$ -soft nuclei,  $^{190}\text{W}_{116}$  [12] and  $^{192}\text{Os}_{116}$  [13]. In the case of  $^{172}\text{Dy}$ , however, the  $K^\pi = 8^-$  isomer reveals the robust nature of an axially deformed nucleus, as mentioned in the previous paragraph. In this context, it is unlikely that the observed fall of the  $\gamma$ -vibrational states in  $^{172}\text{Dy}$  is ascribed to the macroscopic effect of axial asymmetry, regardless of its nature being either large amplitude  $\gamma$ -soft dynamics or static triaxiality. This conjecture is supported by inspection of the g.s. rotational band; the  $4_1^+$  state at 251 keV is sufficiently lower than the extrapolated  $2_\gamma^+$  state at 671 keV, being at variance with the well-known feature of an axially-asymmetric rotor, in which these states are nearly degenerate. Furthermore, the energy ratio  $R_{4/2} = E(4_1^+)/E(2_1^+) = 3.30$  for  $^{172}\text{Dy}$  remains close to the limit for a symmetric rotor (3.33). Thus, all these arguments point to an axially-symmetric structure for  $^{172}\text{Dy}$ .

The extrapolated energy of the  $2_\gamma^+$  state in  $^{172}\text{Dy}$  is the lowest of the known  $\gamma$ -vibrational band heads in the even-even Dy isotopes. To understand the underlying mechanism of the observed lowering of the  $\gamma$ -vibrational band, we have performed model calculations based on a Skyrme energy-density-functional (EDF) [14]. With the use of the SkM\* functional, the ground states are calculated by the Hartree-Fock-Bogoliubov (HFB) method, while the Quasiparticle Random-Phase Approximation (QRPA) is employed for the intrinsic excitations.

As demonstrated in Fig. 2(c), the HFB+QRPA calculation reproduces the experimental results very well, in particular the decreasing trend of the  $2_\gamma^+$  energies from  $^{170}\text{Dy}$  to  $^{172}\text{Dy}$ . This can be interpreted in terms of the 2qp components involved in the QRPA wave functions, which satisfy the selection rules of the asymptotic quantum number for the non-axial quadrupole matrix element [15]. Concerning the proton configurations, the  $\pi 1/2^+[411] \otimes \pi 3/2^+[411]$  and  $\pi 1/2^+[411] \otimes \pi 5/2^+[413]$  components play an important role in generating the  $\gamma$  vibration for the Dy isotopes considered in Fig. 2(c). Since the amplitude squared of these proton components, 0.25 and 0.19 on average, respectively, does not change so much with the neutron number, the energy variation of the  $2_\gamma^+$  states depends mainly on the neutron configuration. As exhibited in Fig. 2(d), the  $\nu 1/2^- [510] \otimes \nu 5/2^- [512]$  component dominates the neutron wave function in  $^{170}\text{Dy}$ . While the amplitude of this neutron 2qp component decreases as the neutron number increases, the other two components,  $\nu 3/2^- [512] \otimes \nu 7/2^- [514]$  and  $\nu 3/2^- [512] \otimes \nu 1/2^- [510]$ , become significant aspects of the neutron wave function instead. In  $^{172}\text{Dy}$ , it is expected that a coherent superposition of these three neutron excitations gives rise to the enhancement of  $\gamma$  vibration, resulting in the lowered  $2_\gamma^+$  energy. The quadrupole transition strength to the  $\gamma$ -vibrational mode is predicted to be larger for the neutron excitation than for proton [14]. Thus, the details of the microscopic wave function are crucial for understanding the collectivity in this doubly mid-shell region.

The HFB+QRPA calculation suggests that the  $2_\gamma^+$  state has an even lower energy in  $^{174}\text{Dy}_{108}$  [14], which was unreachable in the present experiment. The predicted energy (0.33 MeV) is lower than the  $2_\gamma^+$  energies of the  $N = 116$  isotones,  $^{190}\text{W}$  and  $^{192}\text{Os}$ , which are known to have the  $\gamma$ -soft nature. Of great interest will be to investigate the collectivity further beyond the neutron midshell in future experiments using more intense RI beams.

## References

- [1] H. Watanabe *et al.*, Phys. Lett. B 760, 641 (2016)
- [2] G.D. Dracoulis *et al.*, Phys. Lett. B 635, 200 (2006)
- [3] G.D. Dracoulis, Phys. Scr. 2013, 014015 (2013)
- [4] N. Fukuda *et al.*, Nucl. Instrum. Methods B 317, 323 (2013)
- [5] S. Nishimura, Prog. Theor. Exp. Phys., 03C006 (2012)
- [6] G. Alaga, Phys. Rev. 100, 432 (1955)
- [7] J. Fujita, Phys. Rev. C 1, 2060 (1970)
- [8] C.J. Gallagher and S.A. Moszkowski, Phys. Rev. 111, 1282 (1958)
- [9] K. Becker *et al.*, Nucl. Phys. A 522, 557 (1991)
- [10] G.D. Dracoulis *et al.*, Phys. Rev. C 81, 054313 (2010)
- [11] F.G. Kondev *et al.*, At. Data and Nucl. Data Tables 103-104, 50 (2015)
- [12] G.J. Lane *et al.*, Phys. Rev. C 82, 051304 (2010)
- [13] G.D. Dracoulis *et al.*, Phys. Lett. B 720, 330 (2013)
- [14] K. Yoshida and H. Watanabe, Prog. Theor. Exp. Phys., 2016, 123D02 (2016)
- [15] B.R. Mottelson and S.G. Nilsson, Mat. Fys. Skr. Dan. Vid. Selsk. 1, No. 8 (1959)